HTD-Vol. 181, Fundamentals of Forced
Convection Heat Transfer
ASME 1991

INFLUENCE OF HYDRODYNAMIC DISPERSION ON CONVECTION ONSET OF A POROUS LAYER WITH VOLUMETRIC HEATING

P. Adnani, I. Catton, and M. A. Abdou
Department of Mechanical, Aerospace and Nuclear Engineering
University of California
Los Angeles, California

ABSTRACT

Onset of natural convection in a horizontally unbounded porous layer with internal heat generation is investigated. The effects of hydrodynamic dispersion on the critical Rayleigh number is determined by introducing an effective medium conductivity which depends linearly on the magnitude of filtration velocity. Various velocity and temperature boundary conditions at the lower and upper surfaces were investigated and it was found that the velocity boundary condition does not affect the convection onset when dispersion is included. Dispersion was shown to reduce the critical Rayleigh number of the layer when volumetric heating is present. This reduction is a function of the bed coarseness or bead diameter/layer thickness ratio.

NOMENCLATURE

a - wave number
A_m - coefficient defined in Eq. 22
b - parameter defined in Eq. 24
B_m, C_m, D_m, E_m - coefficients defined in Appendix I
C_p - specific heat
d - bead diameter

D - $\frac{\partial}{\partial z}$

Da - Darcy number $\frac{\gamma}{L^2}$

$\hat{e}$ - unit vector

F - inertia resistance coefficient $\frac{1.75d}{150(1-\epsilon)}$

$\vec{g}$ - gravitational vector G_m - Eigenvector amplitudes
$\underline{I}$ - integrals defined in Appendix II
J,K,L,M,N - matrices in Eq. 29
k - thermal conductivity
L - layer thickness
$\underline{P}$ - pressure
P,Q - matrices defined in Eq. 30,31

Pr - medium Prandtl number $\frac{(\nu\rho C_p)_f}{k_o}$

Q_v - volumetric heating rate

R - $\frac{g\omega T_r L^3}{\nu\alpha_o}$

Ra_E - External Rayleigh number $\frac{g\omega(T_L-T_U)L^3}{\nu\alpha_o}$

Ra_i - Internal Rayleigh number $\frac{g\omega Q_v L^5}{\alpha_o \nu k_o}$

$\tilde{Ra}$ - Darcy modified Rayleigh number (RaDa)
T - temperature
ΔT - temperature gradient (T_L-T_U)
u,v,w - velocity components in x,y,z direction
$\vec{V}$ - velocity vector
x,y,z - coordinate axes

α - thermal diffusivity $\frac{k}{(\rho C_p)_f}$

β_n - $2n\pi$

γ - permeability $\frac{d^2\epsilon^3}{150(1-\epsilon)^2}$

ϵ - porosity

ζ - dispersivity $\frac{0.43}{1-\epsilon}\frac{d}{L}$

θ, Θ - temperature perturbation

λ - wavelength $\frac{2\pi}{a}$

μ - fluid dynamic viscosity
ν - fluid kinematic viscosity
Π - pressure perturbation
ρ - density
Φ - temperature perturbation amplitude
χ - parameter defined in Eq. A.1
ω - coefficient of thermal expansion for fluid

Ω - $\frac{(\rho C_p)_o}{(\rho C_p)_f}$

subscripts and superscripts

' - dimensionless quantity
~ - Darcy modified
c - critical
e - effective value for medium with flow
f - fluid
L - lower surface
o - effective value for medium with no flow
r - reference value
U - upper surface
x,y,z - coordinate axis

INTRODUCTION

Natural convection in a fully saturated porous layer with internal heat generation has been investigated in the past because of its importance in nuclear reactor safety and geophysical situations. Heat removal rate from a nuclear debris bed after an accidental reactor meltdown; heat transfer within earth's crust, or from buried nuclear waste are just a few examples where thermal convection plays a major role.

The onset of natural convection in a horizontally unbounded porous layer with internal heat generation is the subject of this paper; because of the large volume of literature in this area, only a few of these will be mentioned here. Lapwood (1948) and Horton and Rogers (1945) were the first to look at thermal convection onset in a porous layer subjected to a de-stabilizing temperature gradient, but they did not consider volumetric heating in their investigation. Gasser and Kazimi (1976) performed the linear stability analysis of a volumetrically heated porous layer with and without an imposed temperature gradient. Although their analysis determined a critical Rayleigh number for a porous layer, it did not account for the effects of hydrodynamic dispersion on the convection onset. Various convective planforms for this problem were studied by Tveitereid (1977) who suggested that for small disturbances after the onset, 2-dimensional rolls are stable planforms for this problem. Somerton and Catton (1982) investigated the stability problem of a volumetrically heated porous layer overlaid by a fluid. Their analysis showed the thickness of the overlaid fluid to be an important parameter influencing the convection onset. Recently, Prasad (1987) and Haajizadeh et al. (1984) have looked at the effects of sidewalls on heat transfer in a vertical cavity subjected to internal heat generation.

All of the above studies are based on the equations describing Darcy flow with an effective mixture thermal conductivity in the energy equation. The key shortcoming in all of them has been the absence of hydrodynamic dispersion from the governing equations. It is the impact of the hydrodynamic dispersion that will be addressed here. Hydrodynamic dispersion has been shown to be an important mechanism influencing heat transfer in forced convection flows by Cheng and Vortmeyer (1988), Hunt and Tien (1988), and natural convection flows by Georgiadis and Catton (1988) and Kvernvold and Tyvand (1980) in porous media.

The effects of dispersion on the onset of convection, in terms of a critical Rayleigh number (Ra_{k_e}), in a volumetrically heated porous layer will be investigated in this paper. It should be noted that for a porous layer with only a de-stabilizing temperature gradient, Neischloss and Dagan (1975) have shown the convection onset to be independent of hydrodynamic dispersion. However, in a porous layer with volumetric heating, He and Georgiadis (1990) have suggested that dispersion does influence the convection onset. The main difference between the two problems is that the conductive state temperature profile is non-linear for the latter case while it is linear when a temperature gradient is imposed on the boundaries. The non-linear temperature gradient leads to a first order interaction with the filtration velocity. A first order stability analysis of this problem will be performed and dispersion will be included in the energy equation. Various velocity and temperature boundary conditions will be examined. The results from this work can be used, in part, to explain the observed scatter in the experimental data of Hardee and Nilson (1977), Rhee, Dhir and Catton (1978), and Kulacki and Freeman (1979).

GOVERNING EQUATIONS

The porous layer shown in Fig. 1 is at a conductive state when the magnitude of volumetric heating is sufficiently small. The temperature distribution $T_0(z)$ for this case can be derived by solving the 1-D conduction equation at steady state

$$\frac{d^2T_0}{dz^2}+\frac{Q_v}{k_0}=0 \tag{1}$$

If the lower and upper surfaces are both isothermal then

$$T_0(z) = -\frac{Q_v}{2k_0}z^2+\left(\frac{T_U-T_L}{L}+\frac{Q_vL}{2k_0}\right)z+T_L \tag{2}$$

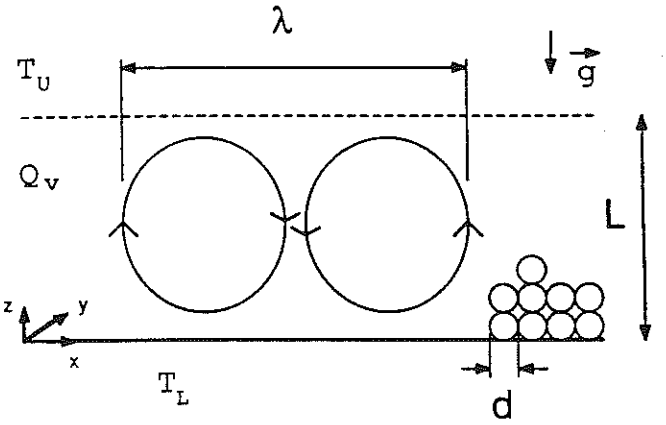

Fig. 1: Diagram of porous layer with volumetric heating.

If the lower surface is adiabatic and the upper surface is isothermal

$$T_0(z) = -\frac{Q_v}{2k_0}(z^2-L^2)+T_U \tag{3}$$

In this analysis both conditions will be investigated. As the volumetric heating rate is increased, the fluid at the lower portion of the layer becomes hotter (and less dense) than the fluid overlaying it, and eventually the system departs to a convective state. For small disturbances from this equilibrium conductive state, velocity and temperature are given by

$$\vec{V} = u\hat{e}_x+w\hat{e}_z \tag{4}$$

$$T=T_0(z)+\theta(x,y,z) \tag{5}$$

The convection planform after the onset is assumed to be 2-Dimensional rolls. After onset, the equations governing natural convection in the porous layer become

$$\nabla\cdot\vec{V} = 0 \tag{6}$$

$$-\nabla P+\rho\vec{g}+\mu\nabla^2\vec{V} -\frac{\mu}{\gamma}\vec{V} -\rho\frac{F}{\gamma}|\vec{V}|\vec{V} =0 \tag{7}$$

$$(\rho C_p)_f\vec{V}\cdot\nabla T=\nabla\cdot(k_e\nabla T)+Q_v \tag{8}$$

The transient terms ($\partial/\partial t$) have been dropped because, near the onset, convective motion is marginally stable as suggested by Gasser and Kazimi (1976). The last term on the left hand side of Eq. 7 is known as the Forchheimer term and represents inertial drag in porous matrices. This term becomes important when superficial velocities are high ($Re > 10$). It will be dropped from our analysis because it is a second order term and our objective is to do a linear stability analysis. The effective medium conductivity (k_e) has a stagnant (k_0) and a dispersive component

$$k_e=k_0+\frac{0.43}{1-\varepsilon}d(\rho C_p)_f|\vec{V}| \tag{9}$$

The stagnant component may be calculated from the method suggested by Adnani et al. (1989) while the dispersive component is estimated by the statistical technique of Georgiadis and Catton (1988). After invoking the Boussinesq approximation and combining the hydrostatic pressure gradient with the buoyant term, one can non-dimensionalize the governing equations with L, ν/L, $\rho(\nu/L)^2$ and T, for length, velocity, pressure, and temperature respectively. Next substitute Eq.'s 5 and 9 into Eq. 8, neglect the second order terms from the energy equation, and take $\hat{e}_y\cdot(\nabla\times\nabla\times$ momentum) to get

$$\frac{\partial u'}{\partial x'}+\frac{\partial w'}{\partial z'}=0 \tag{10}$$

$$-\frac{R}{Pr}\nabla_1^2\theta'-\nabla^4 w'+\frac{1}{Da}\nabla^2 w'=0 \tag{11}$$

For isothermal/isothermal surfaces

$$w'\frac{Pr}{R}\left[Ra_I\left(\frac{1}{2}-z'\right)-Ra_E\right]-\nabla^2\theta'+\zeta\frac{Pr}{R}\left\{\begin{matrix}D|\vec{W}'|\left[Ra_I\left(\frac{1}{2}-z'\right)-Ra_E\right]\\-\vec{W}'|Ra_I\end{matrix}\right\} \tag{12}$$

For an adiabatic/isothermal condition

$$-w'\frac{Pr}{R}\left[Ra_I z'\right]-\nabla^2\theta'-\zeta\frac{Pr}{R}\left[D|\vec{W}'|Ra_I z'-\vec{W}'|Ra_I\right] \tag{13}$$

The primes denote dimensionless parameters and will be dropped from here on for simplicity. ζ is the dispersivity of the porous medium and is linearly proportional to bead diameter/layer thickness (d/L) ratio. It is proportional to bead diameter (d) because dispersion depends linearly on the bead size, and it is inversely proportional to L because the velocity was scaled using ν/L. This means that the magnitude of dispersive term in the energy equation depends on the parameter d/L. Once again note that both internal (Ra_I) and external (Ra_E) heating can be present simultaneously. The operator ∇_1^2 is defined as

$$\nabla_1^2=\frac{\partial^2}{\partial x^2}+\frac{\partial^2}{\partial y^2} \tag{14}$$

To analyze the parameters into normal modes, the following perturbations of $\vec{V}$ and θ will be introduced

$$\vec{V}(x,y,z)=\vec{V}(z)\exp[i(a_x x+a_y y)] \tag{15}$$

$$\theta(x,y,z)=\Theta(z)\exp[i(a_x x+a_y y)] \tag{16}$$

The a's denote wavenumbers in the given directions. If the convective planform has the form of 2-dimensional rolls, the wavelength in the y-direction is infinitely long and the wavenumber in that direction is zero ($a_y=0$). The gradient operators can then be re-written as

$$a^2=a_x^2+a_y^2=a_x^2 \tag{17}$$

$$\nabla_1^2=-a^2 \tag{18}$$

$$\nabla^2=D^2-a^2 \tag{19}$$

After applying these operators to Eq.'s 11-12 and rearranging, one may write the momentum perturbation equation in the form

$$\frac{Pr}{a^2R}(D^2-a^2)\left[D^2-a^2-\frac{1}{Da}\right]W=\Theta \tag{20}$$

The energy equation for the isothermal/isothermal case is

$$W\frac{Pr}{R}\left\{\begin{matrix}Ra_I\left(\frac{1}{2}-z\right)\\-Ra_E\end{matrix}\right\}-\left\{\begin{matrix}\zeta\frac{Pr}{R}\left[D|\vec{V}|\left[Ra_I\left(\frac{1}{2}-z\right)-Ra_E\right]-|\vec{V}|Ra_I\right]\\+(D^2-a^2)\Theta\end{matrix}\right\} \tag{21}$$

For the adiabatic/isothermal case the energy equation is different

$$-W\frac{Pr}{R}[Ra_I z]-(D^2-a^2)\Theta-\zeta\frac{Pr}{R}\left(D|\vec{V}|Ra_I z+|\vec{V}|Ra_I\right) \tag{22}$$

Once the continuity equation is used to relate U and W,

$$U=\frac{i}{a_x}DW \tag{23}$$

the 2-D velocity norm and its gradient can be determined

$$\vec{W}|=\sqrt{|U|^2+|W|^2}=\sqrt{\left(\frac{DW}{a_x}\right)^2+W^2} \tag{24}$$

$$D|\vec{V}|=\left[W^2+\left(\frac{DW}{a_x}\right)^2\right]^{-\frac{1}{2}}\left[WDW+\frac{(DW)(D^2W)}{a_x^2}\right] \tag{25}$$

METHOD OF SOLUTION

The solution to Eqs. 20-22 will be approximated using the Galerkin method. The temperature perturbation (Θ) is represented by a Fourier sine series when both surfaces are isothermal

$$\Theta=\frac{1}{a^2}\sum_m G_m\sin(\beta_m z) \tag{26}$$

where

$$\beta_m=m\pi \tag{27}$$

If the lower surface is adiabatic and the upper surface is isothermal, a different series solution is needed

$$\Theta=\frac{1}{a^2}\sum_m G_m\cos(\tau_m z) \tag{28}$$

with

$$\tau_m=\frac{2m-1}{2}\pi \tag{29}$$

Substitution of the above into Eq. 20 yields the particular solution for the velocity perturbation (W)

$$W=\sum_m A_m F_m \tag{30}$$

where

$$A_m=\frac{\frac{R}{Pr}}{\left(\kappa_m^2+a^2\right)^2+\frac{\kappa_m^2+a^2}{Da}}G_m \tag{31}$$

$$\begin{array}{ll} \text{if isothermal/isothermal} & F_m=\sin(\beta_m z)\ ,\ \kappa_m=\beta_m \\ \text{if adiabatic/isothermal} & F_m=\cos(\tau_m z)\ ,\ \kappa_m=\tau_m \end{array} \quad (32)$$

The general solution for W is obtained by adding the homogeneous and particular solutions of W

$$W=\sum_m A_m \begin{bmatrix} F_m+B_m\sinh(az)+C_m\sinh(bz) \\ +D_m\cosh(az)+E_m\cosh(bz) \end{bmatrix} \quad (33)$$

with

$$b^2=a^2+\frac{1}{Da} \quad (34)$$

The constants B_m through E_m can be evaluated by applying the velocity boundary conditions to the general solution of W. These boundary conditions are

$$\begin{array}{ll} W=DW=0 & \text{for rigid boundaries} \\ W=D^2W=0 & \text{for free boundaries} \end{array} \quad (35)$$

Applying these conditions to Eq. 33 and using Cramer's rule, one can evaluate B_m through E_m. The results are shown in Appendix I for various rigid/free surface combinations. Substituting the expression for W given by Eq. 33 into Eq. 21, multiplying by sin(nπz) and integrating from z=0 to 1 yields the following characteristic equation for the isothermal/isothermal condition

$$\left\{ \begin{array}{c} Ra_I\sum_m A_m\left[\frac{I_o}{2}-I_5+B_m\left(\frac{I_1}{2}-I_6\right)+C_m\left(\frac{I_2}{2}-I_7\right)+D_m\left(\frac{I_3}{2}-I_8\right)+E_m\left(\frac{I_4}{2}-I_9\right)\right] \\ +Ra_E\sum_m A_m\left[-I_o-B_mI_1-C_mI_2-D_mI_3-E_mI_4\right]+\sum_m\left(\frac{\beta_m^2}{a^2}+1\right)G_mI_o \\ +\zeta\left[Ra_I\left(-\frac{1}{2}I_{10}+I_{11}+I_{12}\right)+Ra_EI_{10}\right] \end{array} \right\}=0 \quad (36)$$

For the adiabatic/isothermal condition, the solution for W is substituted into Eq. 22 instead, and the result is multiplied by cos(nπz). After integrating between 0 to 1, one obtains the characteristic equation

$$\left\{ \begin{array}{c} Ra_I\sum_m A_m\left[-I_{14}-B_mI_{15}-C_mI_{16}-D_mI_{17}-E_mI_{18}\right] \\ +\sum_m\left(\frac{\tau_m^2}{a^2}+1\right)G_mI_{13}+\zeta\left[Ra_I(I_{19}+I_{20})\right] \end{array} \right\}=0 \quad (37)$$

The I_n's are integrals defined in Appendix II. It should be noted that I_{10}, I_{11}, I_{12}, I_{19}, I_{20} represent the contributions of hydrodynamic dispersion. For simplicity, the characteristic equations are written in matrix form

$$Ra_I\bar{M}\bar{G}+Ra_E\bar{N}\bar{G}+\bar{L}\bar{G}+\zeta\left(Ra_I\bar{J}+Ra_E\bar{K}\right)=\bar{0} \quad (38)$$

where $\bar{L}$, $\bar{M}$, $\bar{N}$ are n x n matrices, $\bar{G}$ is the eigenvector, and $\bar{J}$ and $\bar{K}$ are column matrices resulting from the hydrodynamic dispersion terms. For the adiabatic/isothermal case Ra_E is always zero. After combining Eqs. 24,25,33, one can factor out G_k to yield

$$\bar{J}=\bar{P}\bar{G} \quad (39)$$

$$\bar{K}=\bar{Q}\bar{G} \quad (40)$$

$\bar{P}$ and $\bar{Q}$ are n x n matrices with all zero elements except the k^{th} column, and G_k is the largest eigenvector amplitude. This modification allows us to combine the dispersive terms with the other terms in Eq. 38. The result is

$$\left[Ra_I(\bar{M}+\zeta\bar{P})+Ra_E(\bar{N}+\zeta\bar{Q})+\bar{L}\right]\bar{G}=\bar{0} \quad (41)$$

Once again Ra_E is zero for the adiabatic/isothermal case. To solve this eigenvalue problem the following steps are taken:

1) Solve the eigenvalue problem (Eq. 41) with $\zeta=0$ (no dispersion)
2) Evaluate the dispersive terms from Eq. 24-25
3) Determine $\bar{P}$ and $\bar{Q}$ from (39-40)
4) Solve the eigenvalue problem with hydrodynamic dispersion.
5) Go to step 2 and iterate until convergence.

RESULTS FOR THE ISOTHERMAL/ISOTHERMAL CASE

The solution to Eq. 41 is determined by a tenth order (n=10) approximation. Fig. 2 shows the dependence of critical Rayleigh number on the number of terms in the expansion. Increasing the number of terms from 10 to 11 changes the result by only 0.1%; therefore, a 10 term expansion will be used here. To check the model validity, results without dispersion were compared against the results of Gasser and Kazimi (1976). They had shown the convection onset of various porous layers to fall on a single curve if the critical Darcy-Rayleigh numbers (Ra_c×Da) are plotted. Fig. 3 shows the effect of dispersion on $\bar{Ra}_c$ for a rigid/free porous layer with d/L=0.05. As shown by Neischloss and Dagan (1975), $\bar{Ra}_{E_c}$ is not influenced by hydrodynamic dispersion when volumetric heating is absent. On the other hand $\bar{Ra}_{I_c}$ is effected; its magnitude is reduced meaning the porous layer becomes more unstable when dispersion is present. The influence of dispersion is also shown when various stabilizing and de-stabilizing temperature gradients ($\bar{Ra}_{E_c}$) are imposed on the layer.

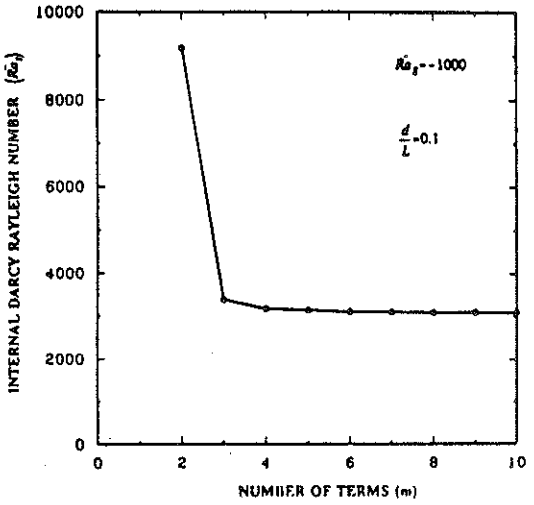

Fig. 2: Plot of Darcy-Rayleigh number vs. number of terms of Galerkin approximation.

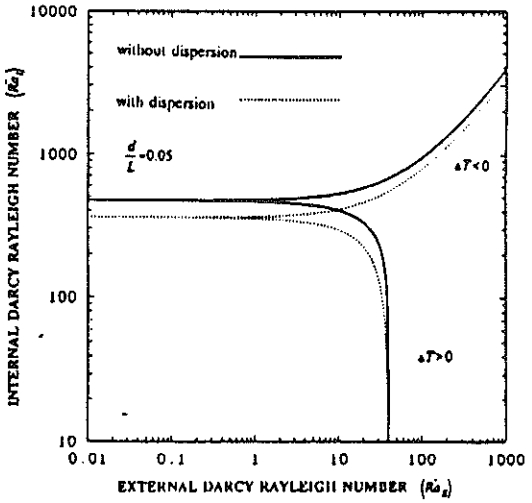

Fig. 3: Stability curve for a rigid/free layer.

It was mentioned earlier that, in the absence of hydrodynamic dispersion, the critical Darcy-Rayleigh numbers can be plotted on a single curve. This is not the case when dispersion is present. The difference between the two cases can be attributed to the dispersivity parameter ς which is directly proportional to d/L, meaning one curve cannot represent various porous layers with different bead diameter to layer thickness ratios. To observe the importance of the dispersivity parameter ς, the stability curve for a rigid/free layer with d/L=0.1 is plotted in Fig. 4. As the layer becomes coarser (d/L is increased), the influence of dispersion becomes more significant and $\widetilde{Ra}_{l_c}$ is further reduced. Because the volume averaging techniques used to derive the conservation equations and the dispersion model used in this work are valid only for d/L~O(1), no attempt will be made to determine $\widetilde{Ra}_{l_c}$ outside of this region.

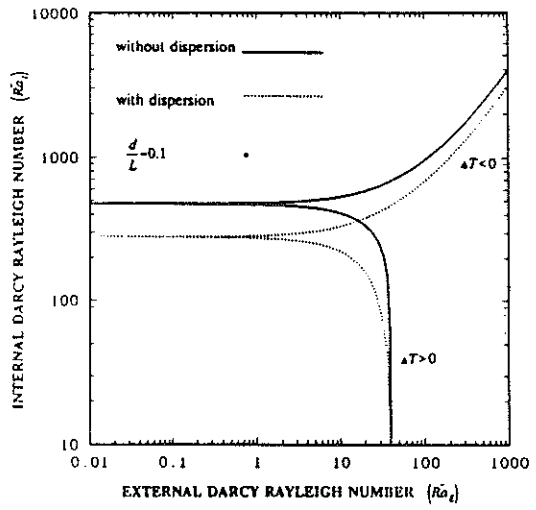

Fig. 4: Stability curve for a rigid/free layer.

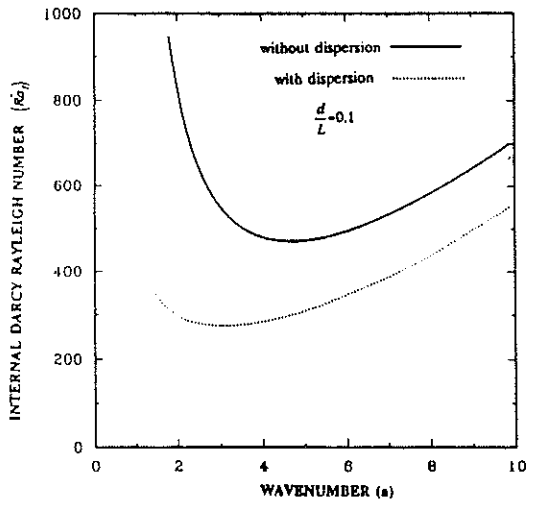

Fig. 5: Plot of Darcy-Rayleigh number vs. horizontal wavenumber.

In addition to changing the critical Rayleigh number of a volumetrically heated porous layer, hydrodynamic dispersion also affects the size of the 2-D rolls. Fig. 5 shows the relationship between the wavenumbers and $\widetilde{Ra}_l$ in the absence of external heating. The effective wavenumber is the value corresponding to the minimum $\widetilde{Ra}_l$ (which is also the critical Rayleigh number $\widetilde{Ra}_{l_c}$). Dispersion reduces the effective wavenumber at the onset of convection. A reduction of the effective wavenumber translates to an increase in the size of the 2-D rolls. Physically, wavelength expansion makes sense because dispersion enhances the spreading of fluid in the interstitial pores and

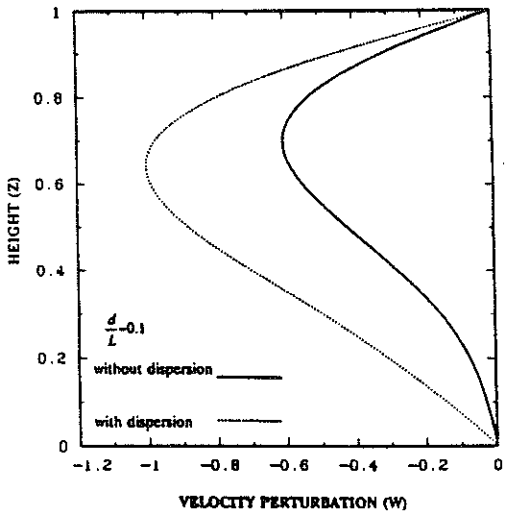

Fig. 6: Influence of Dispersion on normalized perturbation velocity.

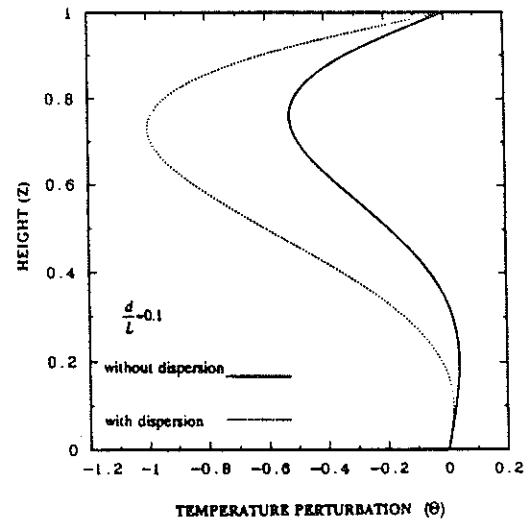

Fig. 7: Influence of dispersion on normalized perturbation temperature.

one would expect this spreading to increase the size of the convective rolls. The effects of dispersion on the normalized perturbation functions W and Θ can be observed in Figs. 6 and 7.

So far attention has only been focused on a porous layer with a rigid lower surface and a free upper surface. Lapwood (1948) and Gasser and Kazimi (1976) have stated that, in a porous layer, the presence of a solid or a rigid surface does not affect the convection onset. This may seem surprising at first because $\widetilde{Ra}_{l_c}$ of the analogous problem in a nonporous layer depends strongly on whether the boundaries are rigid or free. In a porous layer, however, an order of magnitude analysis of the momentum equation shows the Darcian term to be much larger than the Brinkman term which represents the viscous effects near a solid wall. This means the frictional forces in the interstitial pores are much larger than the frictional losses at the solid boundaries. As an exercise the stability curves for a rigid/rigid condition with and without dispersion are plotted in Figs. 8 and 9. Comparison of these curves with Fig. 3 and 4 verifies the fact that the onset does not depend on whether the boundary is rigid or free. The temperature boundary condition, however, does influence the onset significantly as will be shown in the next section.

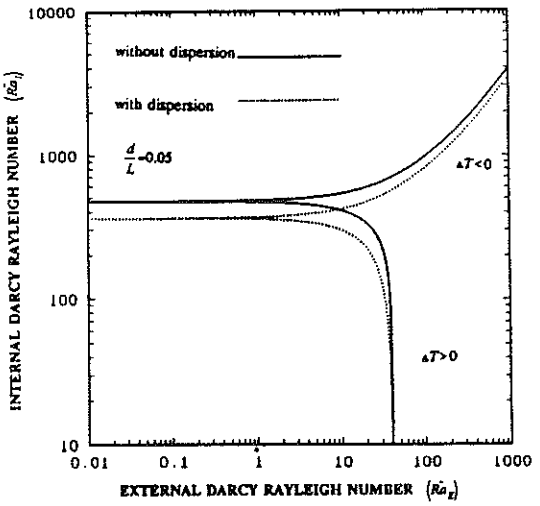

Fig. 8: Stability curve for a rigid/rigid layer.

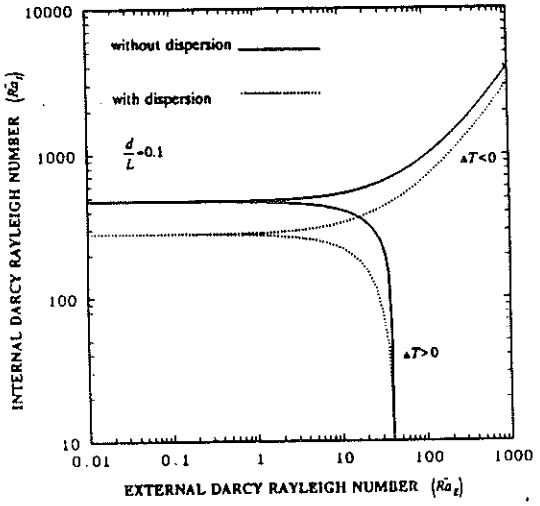

Fig. 9: Stability curve for a rigid/rigid layer.

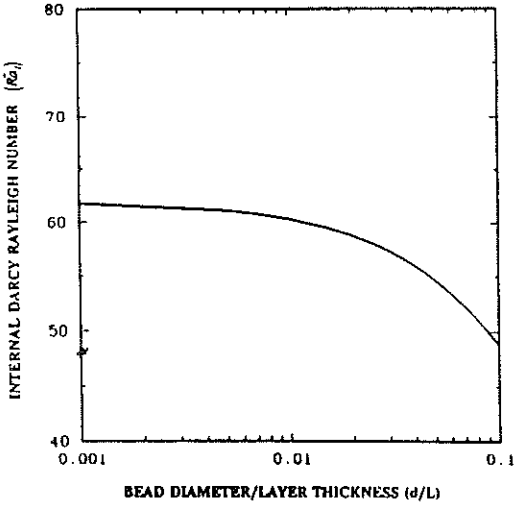

Fig. 10: Plot of critical Darcy-Rayleigh number vs. bed coarseness.

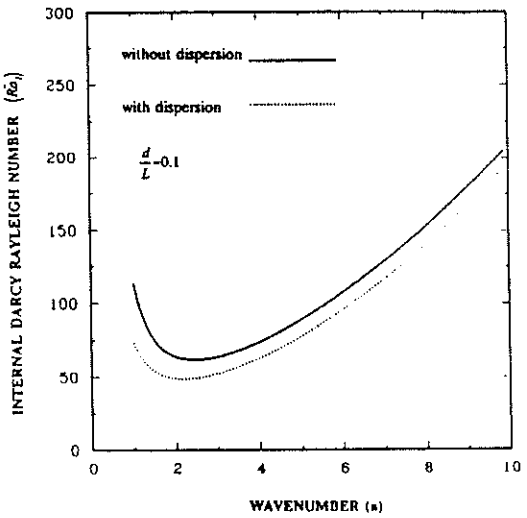

Fig. 11: Plot of Darcy-Rayleigh number vs. horizontal wavenumber.

RESULTS FOR THE ADIABATIC/ISOTHERMAL CASE

Unlike the isothermal/isothermal case which, to our knowledge, has not been investigated experimentally, the adiabatic/isothermal condition has been studied by several authors including Buretta and Berman (1976), Hardee and Nilson (1977), Rhee, Dhir and Catton (1978), and Kulacki and Freeman (1979). These investigations have shown the measured critical Rayleigh number to vary sometimes by as much as 40%. For example Buretta and Berman (1976) and Hardee and Nilson (1977) determined $\bar{Ra}_{ic}$ to be 66 while Rhee, Dhir and Catton have reported this quantity to be 92. (Note, the critical Rayleigh number defined by these authors is half of the Darcy-Rayleigh number defined here. These values were modified to be consistent with $\bar{Ra}_{ic}$ here). Factors such as non-uniformity of volumetric heating in the particle bed, and whether the lower surface is completely adiabatic or not have been suggested as an explanation for this scattering behavior.

We propose dispersion to be an important factor that can explain some of this scatter. For simplicity, a free/free velocity boundary condition will be used here because the onset is independent of the type of velocity boundary condition imposed. Fig. 10 shows how the convection onset is affected when d/L is changed. The critical Darcy-Rayleigh number is reduced 26% (from 62 to 49) when d/L is increased from 0.001 to 0.1. Once again the effective wavenumber is reduced (see Fig. 11). Note that results from this analysis tend to be somewhat lower than what Rhee, Dhir and Catton (1978) have measured, but the result for weak dispersion (small d/L) is only 10% lower than the measurements of Buretta and Berman (1976) and Hardee and Nilson (1977). There are several explanations for the difference between our predictions and their measurements. First, the onset is very sensitive to the temperature boundary conditions. In the absence of dispersion, $\bar{Ra}_{ic}$ is 480 for the isothermal/isothermal condition and 66 for the adiabatic/isothermal condition. Therefore, future experiments must attempt to minimize heat losses from adiabatic surfaces. Second, $\bar{Ra}_{ic}$ is determined by interpolating the Nusselt numbers before and after the onset; more finely tuned measurements near the onset may be necessary to increase the accuracy of data. Table 1 shows the summary of results for several cases which were studied.

Lower/Upper boundaries		d/L		
		0.01	0.05	0.1
rig/rig iso/iso	$\tilde{Ra}_{lc}$	446	361	278
	a_c	4.5	3.7	3.1
rig/free iso/iso	$\tilde{Ra}_{lc}$	446	360	276
	a_c	4.5	3.7	3.1
free/free adi/iso	$\tilde{Ra}_{lc}$	60	55	49
	a_c	2.4	2.3	2.2
rig/rig adi/iso	$\tilde{Ra}_{lc}$ measured	66-92		

Table 1: Summary of Critical Rayleigh numbers

CONCLUSIONS

The influence of hydrodynamic dispersion on the convection onset of a horizontally unbounded porous layer with internal heat generation was determined by performing a linear stability analysis. Dispersion was represented by a term which depends linearly on the magnitude of the filtration velocity. The convection planform after the onset was assumed to be 2-dimensional rolls.

It was shown that Ra_{lc} is reduced in the presence of dispersion, meaning that the porous layer has become more unstable. Additionally, this reduction of Ra_{lc} becomes more significant as the porous layer becomes coarser. This is due to the fact that the dispersivity, which is proportional to the bead diameter/layer thickness, is increased as the layer is made coarser. Analysis of wavenumbers with and without hydrodynamic dispersion showed the size of 2-dimensional rolls to increase when dispersion was included in the energy equation. Physically, this makes sense because dispersion enhances spreading of the fluid and therefore is expected to make the 2-D rolls larger. Stability curves for various d/L ratios and Ra_F were plotted, and it was verified that in the absence of internal heating, convection onset is not influenced by dispersion.

Comparison of stability curves for a rigid/free and a rigid/rigid layer showed that the velocity boundary condition does not effect the onset significantly with or without dispersion. This was expected because the frictional forces due to flow channeling are larger than the viscous forces near solid walls. Since the velocity boundary condition is unimportant, mechanisms such as dispersion damping and flow channelling near solid boundaries do not affect the onset significantly. However, the temperature boundary condition was shown to affect the critical Rayleigh number drastically. Therefore, future experiments with volumetric heating must ensure that the correct temperature boundary condition is imposed on the boundaries.

ACKNOWLEDGEMENTS

This work was supported by the U.S. Department of Energy under contracts #DE-FG03-86ER52123 and #DE-FG03-86ER14033.

REFERENCES

Adnani, P., Raffray, A.R., Abdou, M.A., Catton, I., "Modeling of Effective Thermal Conductivity for a Packed Bed," *UCLA-FNT-29*, University of California, Los Angeles, 1989.

Buretta, R.J. and Berman, A.S., "Convective Heat Transfer in a Liquid Saturated Porous Layer," *(ASME) J. Heat Transfer*, Vol. 98, 249-253, 1976.

Cheng, P. and Vortmeyer, P., "Transverse Thermal Dispersion and Wall Channeling in a Packed Bed with Forced Convective Flow," *Chem. Eng. Sci.*, Vol. 43, No. 9, 2523-2532, 1988.

Gasser, R.D. and Kazimim M.S., "Onset of Convection in a Porous Medium with Internal Heat Generation," *ASME Trans. J. Heat Transfer*, Vol. 98, 49-54, 1976.

Georgiadis, J.G. and Catton, I. "Dispersion in Cellular Thermal Convection in Porous Media," *Int. J. Heat Mass Transfer*, Vol. 31, 1081-1091, 1988.

Haajizadeh, M., Ozguc, A.F., and Tien, C.L., "Natural Convection in a Vertical Porous Enclosure with Internal Heat Generation," *Int. J. Heat Mass Transfer*, Vol. 27, No. 10, 1893-1902, 1984.

Hardee, H.C. and Nilson, R.H., "Natural Convection in Porous Media with Heat Generation", *Nuc. Sci. and Eng.*, Vol. 63, 119-132, 1977.

He, X.S. and Georgiadis, J.G., "Natural Convection in Porous Media: Effect of Weak Dispersion on Bifurcation," *J. Fluid Mech.*, Vol. 216, 285-298, 1990.

Horton, C.W. and Rogers Jr., F.T., "Convection Currents in a Porous Medium," *J. Appl. Phys.*, Vol. 16, 367-370, 1945.

Hunt, M.L. and Tien, C.L., "Non-Darcian Convection in Cylindrical Packed Beds," *ASME Trans. J. Heat Transfer*, Vol. 110, 378-384, 1988.

Jeffreys, H., "The Stability of a Layer of Fluid Heated Below," *Phil. Mag.*, Vol. 2, 833-344, 1926.

Kulacki, F.A. and Freeman, R.G., "A Note on Thermal Convection in a Saturated, Heat-Generating Porous Layer," *ASME Trans. J. Heat Transfer*, Vol. 101, 169-171, 1979.

Kvernvold, O. and Tyvand, P.A., "Dispersion Effects on Thermal Convection in Porous Media," *J. Fluid Mech.*, Vol. 99, Pt. 4, 673-686, 1980.

Lapwood, E.R., "Convection of a Fluid in a Porous Medium," *Proc. Camb. Phl. Soc.*, Vol. 44, 508-521, 1948.

Neischloss, H. and Dagan, G., "Convective Currents in a Porous Layer Heated from Below: The Influence of Hydrodynamic Dispersion," *Phys. of Fluids*, Vol. 18, No. 7, 757-761, 1975.

Prasad, V., "Thermal Convection in a Rectangular Cavity Filled with a Heat-Generating, Darcy Porous Medium," *ASME Trans. J. Heat Transfer*, Vol. 109, 697-703, 1987.

Rhee, S.J., Dhir, V.K., and Catton, I., "Natural Convection Heat Transfer in Beds of Inductively Heated Particles," *ASME Trans. J. Heat Transfer*, Vol. 100, 78-85, 1978.

Somerton, C.W. and Catton, I., "On the Thermal Instability of Superposed Porous and Fluid Layers," *ASME Trans. J. Heat Transfer*, Vol. 104, 160-165, 1982.

Tveitereid, M., "Thermal Convection in a Horizontal Porous Layer with Internal Heat Sources," *Int. J. Heat Mass Transfer*, Vol. 20, 1045-1050, 1977.

APPENDIX I

The constants B_m through E_m in Eq. 33 can be determined after applying the proper boundary conditions and then using Cramer's rule. For the isothermal/isothermal case with rigid/free condition see Gasser and Kazimi (1976). For the isothermal/isothermal case with a rigid/rigid condition

$$\chi = \left\{ \begin{array}{c} ab\left(\sinh^2 a + \sinh^2 b - \cosh^2 b - \cosh^2 a + 2\cosh a \cosh b\right) \\ -\sinh a \sinh b\left(a^2 + b^2\right) \end{array} \right\}^{-1} \quad \text{(A.11)}$$

$$B_m = \chi \beta_m \left\{ \begin{array}{c} a \sinh a \sinh b - b \cosh a \cosh b - b \sinh^2 b + b \cosh^2 b \\ + b(-1)^m (\cosh a - \cosh b) \end{array} \right\} \quad \text{(A.12)}$$

$$C_m = \chi \beta_m \left\{ \begin{array}{c} b \sinh a \sinh b + (-1)^{m+1} a \cosh a - a \sinh^2 a + a \cosh^2 a \\ + \cosh b\left[(-1)^m a - a \cosh a\right] \end{array} \right\} \quad \text{(A.13)}$$

$$D_m = \chi \beta_m \left\{ \begin{array}{c} b \sinh a \cosh b - a \cosh a \sinh b \\ (-1)^{m+1} (b \sinh a - a \sinh b) \end{array} \right\} \quad \text{(A.14)}$$

$$E_m = -D_m \quad \text{(A.15)}$$

For the adiabatic/isothermal case with free/free surfaces

$$B_m = -\frac{b^2+\tau_m^2}{b^2-a^2}\frac{\cosh a}{\sinh a} \tag{A.16}$$

$$C_m = -\frac{a^2+\tau_m^2}{b^2-a^2}\frac{\cosh b}{\sinh b} \tag{A.17}$$

$$D_m = -\frac{b^2+\tau_m^2}{b^2-a^2} \tag{A.18}$$

$$E_m = -\frac{a^2+\tau_m^2}{b^2-a^2} \tag{A.19}$$

APPENDIX II

The integrals in Eq. 36 (isothermal/isothermal condition) are defined as follows:

$$I_0(m,n) = \int_0^1 \sin(\beta_n z)\sin(\beta_m z)\,dz \tag{A.20}$$

$$I_1(n) = \int_0^1 \sin(\beta_n z)\sinh(az)\,dz \tag{A.21}$$

$$I_2(n) = \int_0^1 \sin(\beta_n z)\sinh(bz)\,dz \tag{A.22}$$

$$I_3(n) = \int_0^1 \sin(\beta_n z)\cosh(az)\,dz \tag{A.23}$$

$$I_4(n) = \int_0^1 \sin(\beta_n z)\cosh(bz)\,dz \tag{A.24}$$

$$I_5(n,m) = \int_0^1 z\sin(\beta_n z)\sin(\beta_m z)\,dz \tag{A.25}$$

$$I_6(n) = \int_0^1 z\sin(\beta_n z)\sinh(az)\,dz \tag{A.26}$$

$$I_7(n) = \int_0^1 z\sin(\beta_n z)\sinh(bz)\,dz \tag{A.27}$$

$$I_8(n) = \int_0^1 z\sin(\beta_n z)\sinh(bz)\,dz \tag{A.28}$$

$$I_9(n) = \int_0^1 z\sin(\beta_n z)\cosh(bz)\,dz \tag{A.29}$$

The analytical solutions to these integrals are given in Gasser and Kazimi (1976). There are also 3 integrals which represent the contribution of hydrodynamic dispersion:

$$I_{10}(n,|\vec{V}|) = \int_0^1 D|\vec{V}|\sin(\beta_n z)\,dz \tag{A.30}$$

$$I_{11}(n,|\vec{V}|) = \int_0^1 |\vec{V}|\sin(\beta_n z)\,dz \tag{A.31}$$

$$I_{12}(n,|\vec{V}|) = \int_0^1 z\,D|\vec{V}|\sin(\beta_n z)\,dz \tag{A.32}$$

These integrals do not have an analytical solution and are evaluated numerically.

For the adiabatic/isothermal case, the integrals in Eq. 37 are defined as follows

$$I_{13}(n,m) = \int_0^1 \cos(\tau_m z)\cos(\tau_n z)\,dz = \begin{cases} 0 \text{ if } n \neq m \\ \frac{1}{2} \text{ if } n = m \end{cases} \tag{A.33}$$

$$I_{14}(n,m) = \int_0^1 z\cos(\tau_n z)\cos(\tau_m z)\,dz = \begin{cases} -\dfrac{1}{(m-n)^2\pi^2} \text{ if } m-n \text{ is odd} \\ -\dfrac{1}{(m+n-1)^2\pi^2} \text{ if } m-n \text{ is even} \\ \dfrac{1}{4} - \dfrac{1}{(2n-1)^2\pi^2} \text{ if } m = n \end{cases} \tag{A.34}$$

$$I_{15}(n) = \int_0^1 z\sinh(az)\cos(\tau_n z)\,dz = \frac{\tau_n \sin\tau_n}{a^2+\tau_n^2}\left[\sinh a - \frac{2a}{a^2+\tau_n^2}\cosh a\right] \tag{A.35}$$

$$I_{16}(n) = \int_0^1 z\sinh(bz)\cos(\tau_n z)\,dz = \frac{\tau_n \sin\tau_n}{b^2+\tau_n^2}\left[\sinh b - \frac{2b}{b^2+\tau_n^2}\cosh b\right] \tag{A.36}$$

$$I_{17}(n) = \int_0^1 z\cosh(az)\cos(\tau_n z)\,dz = \begin{cases} \dfrac{a^2-\tau_n^2}{\left(a^2+\tau_n^2\right)^2} \\ + \dfrac{\tau_n \sin\tau_n}{a^2+\tau_n^2}\left[\cosh a - \dfrac{2a}{a^2+\tau_n^2}\sinh a\right] \end{cases} \tag{A.37}$$

$$I_{18}(n) = \int_0^1 z\cosh(bz)\cos(\tau_n z)\,dz = \begin{cases} \dfrac{b^2-\tau_n^2}{\left(b^2+\tau_n^2\right)^2} \\ + \dfrac{\tau_n \sin\tau_n}{b^2+\tau_n^2}\left[\cosh b - \dfrac{2b}{b^2+\tau_n^2}\sinh b\right] \end{cases} \tag{A.38}$$

The contribution of hydrodynamic dispersion is represented by the following integrals:

$$I_{19}(n,|\vec{V}|) = \int_0^1 |\vec{V}|\cos(\tau_n z)\,dz \tag{A.39}$$

$$I_{20}(n,|\vec{V}|) = \int_0^1 z\,D|\vec{V}|\cos(\tau_n z)\,dz \tag{A.40}$$